Synthesis, Crystal Structure, and Magnetic Order of the Layered Iron Oxycarbonate $Sr_4Fe_2O_6CO_3$

K. Yamaura,*,[1] Q. Huang,†,‡ J. W. Lynn,† R. W. Erwin,† and R. J. Cava†

*Department of Chemistry and Princeton Materials Institute, Princeton University, Princeton, New Jersey 08540; †NIST Center for Neutron Research, National Institute of Standards and Technology, Gaithersburg, Maryland 20899; and ‡Department of Materials and Nuclear Engineering, University of Maryland, College Park, Maryland 20742

The iron oxycarbonate $Sr_4Fe_2O_6CO_3$ is reported. The crystal structure and magnetic order were determined by magnetic susceptibility, powder neutron diffraction, and neutron scattering studies. The structure is tetragonal between 10 and 400 K ($I4/mmm$, $a = 3.88907(4)$ Å and $c = 27.9818(4)$ Å at 295 K), and is related to a 4:3 type Ruddlesden–Popper phase with CO_3 plaques in place of the middle layer of transition metal octahedra. The three-dimensional magnetic ordering transition temperature is 361 K. The magnetic order is antiferromagnetic within the $FeO_2/SrO/SrO/FeO_2$ blocks and ferromagnetic between blocks. © 2000 Academic Press

Key Words: layered oxycarbonates; Ruddlesden–Popper phases; $Sr_4Fe_2O_6CO_3$; powder neutron diffraction; neutron scattering.

1. INTRODUCTION

Transition metal Ruddlesden–Popper(RP)-type compounds often display unusual electronic properties, such as colossal magnetoresistivity, spin–triplet superconductivity, and high-T_c superconductivity (1). Experimental studies on new compounds of this type could help to elucidate the microscopic mechanisms responsible for the unusual properties of the family as a whole. We have recently been studying RP-type phases based on iron oxide to find additional systems showing correlations among magnetic and electric properties and crystal structure.

The general formula for the RP alkaline-earth iron oxide series is $A_{n+1}Fe_nO_{3n+1}$ (A = alkaline-earth ion). At an early stage of our study, we attempted to synthesize the $n = 3$ phase by the procedure reported previously (2). The product obtained by heating at 900°C in nitrogen from a starting mixture of $SrCO_3$ and Fe_3O_4 was found to consist mainly of a tetragonal phase with approximately the same lattice parameters as those reported for "$Sr_4Fe_3O_{10}$" (2). The phase decomposed into SrO and $Sr_3Fe_2O_{7-y}$ by heating at 900°C in air. The relationship between the synthesis conditions and the products is highly reminiscent of what has been observed for the copper oxycarbonate systems (3). Based on the hypothesis that the compound was actually an oxycarbonate, a single-phase compound of the tetragonal phase could reproducibly be obtained from $SrCO_3$ and Fe_3O_4 at the ratio Sr:Fe = 2:1 by heating in mixed gas (10% CO_2 in nitrogen) at 1100°C. A powder neutron diffraction (ND) study on the compound found that the composition of the tetragonal phase is $Sr_4Fe_2O_6CO_3$. Therefore, the $n = 3$ phase previously reported is not an oxide but rather an oxycarbonate. The oxycarbonate phase can also be regarded as a carbon substitution product, $CSr_4Fe_2O_9$, related to $TlSr_4Fe_2O_{9-\delta}$ and $PbSr_4Fe_2O_9$ (4, 5). In this article, the synthesis, crystal structure, and magnetic structure of the iron oxycarbonate are reported.

2. EXPERIMENTAL

The polycrystalline single-phase sample was obtained as follows. A mixture of $SrCO_3$ (99.99%) and Fe_2O_3 (99.99%) with the ratio Sr:Fe = 2:1 was molded into a pellet and heated at 900°C for 12 hours in nitrogen. After the initial heating, grinding, pressing, and heating at 900°C for 36 hours in nitrogen were then repeated three times. Subsequently, the sample was ground, pressed, and heated at 1100°C in mixed gas, 10% CO_2 in nitrogen, for 24 hours, followed by a repeat treatment. Alumina crucibles were employed to hold the pellets.

The magnetic susceptibility was measured at 90 kOe by a commercial apparatus. Thermogravimetric analysis (TGA) was employed to characterize the sample. A heating rate of 2°C/minute to 1000°C in argon was employed. The powder ND data at temperatures between 10 and 400 K were obtained on the BT-1 high-resolution powder diffractometer at the NIST Center for Neutron Research.

A Cu(311) monochromator was employed to produce a monochromatic neutron beam ($\lambda = 1.5401$ Å) with 15′, 20′, and 7′ collimators before and after the monochromator and after the sample, respectively. The intensity of the diffracted neutron beam was measured between 3 and 168 degrees diffraction angles in 0.05 degree steps. Crystal and magnetic structure parameters for the iron oxycarbonate were then refined to a high degree of agreement by calculations with the intensity and angle data employing the program GSAS (6). The neutron scattering amplitudes for the elements in the calculations were set to 0.702, 0.954, 0.665, and 0.581 ($\times 10^{-12}$ cm) for Sr, Fe, C, and O, respectively (6). The BT-2 triple-axis spectrometer was employed

with a pyrolytic graphite PG(002) monochromator ($\lambda = 2.359$ Å) to measure the intensity of the main magnetic peak at temperatures between 30 and 420 K. The evolution of the magnetic scattering was also studied on the BT-2 spectrometer between 200 and 405 K. The statistical uncertainty quoted in all the neutron results represents 1 standard deviation.

3. CRYSTAL STRUCTURE

The initial crystal structure analysis was made on the 400 K ND data. Magnetic ordering contributions to the ND data are absent at this temperature because the
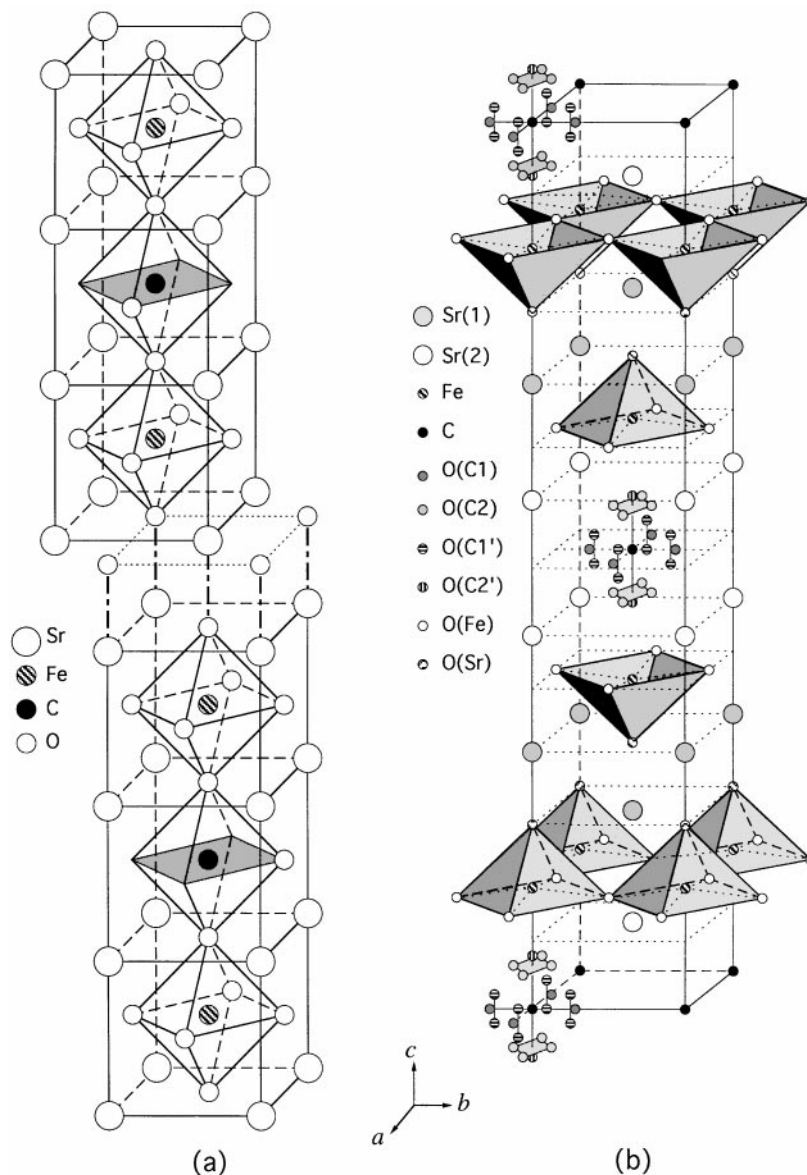

FIG. 1. (a) Initial crystal structure model in the refinement study. (b) Schematic crystal structure view for $Sr_4Fe_2O_6CO_3$ drawn from the final structure parameters at 400 K, showing the randomly occupied oxygen positions around carbon.

collective magnetic order temperature (T_c) is below 400 K. (The details of the analysis of collective magnetic order will be described in the next section.) All of the peaks were indexed by a tetragonal unit cell (*I4/mmm*) with lattice parameters of $a = 3.89530(6)$ Å and $c = 28.0144(5)$ Å. The initial tetragonal structure model is illustrated in Fig. 1a. Each unit cell contains two blocks. The blocks are stacked along the *c*-axis with an origin shift ($\frac{1}{2}a \times \frac{1}{2}b$) and an Sr_2O_2 spacer. Viewed by analogy with the structures of the oxycarbonate copper oxides, a CO_3 triangular plane is expected to be in the center unit of the three nearly cubic units (3). The crystal structures of the related compounds $TlSr_4Fe_2O_{9-\delta}$ and $PbSr_4Fe_2O_9$ also suggest where carbon might be found.

To satisfy the four-fold symmetry operation for the *I4/mmm* space group, one oxygen atom in the carbon layer must be distributed randomly at four positions in the shape of a square (Fig. 1a, shaded). Atomic positions derived from the initial model were employed as initial parameters in the refinement calculations, and a reasonable fit to the observed pattern (400 K) was obtained. The oxygen atoms in the carbon layer, however, were found to have unusually large temperature factors, more than 18 Å^2. This indicates the possibility of positional displacements, or alternatively, complicated orientational disorder of the CO_3 triangles. To solve this problem, a difference Fourier map was made, and four additional oxygen positions (, , 0.05), (0.14, 0, 0.04), (0.28, 0, 0.02), and (0.37, 0, 0) were found. After the four posi-

tions were considered as randomly partially occupied oxygen positions, a significant improvement in the overall fit was obtained. The crystal structure finally obtained, and the fit of the ND data to the model, are shown in Figs. 1b and 2, respectively. The structure model (Fig. 1b) was then employed in refinement calculations for the other temperature data. The lattice parameters vary monotonically with temperature as shown in Fig. 3; there is no structure transition in the studied temperature range. The structure parameters at 295 and 10 K, and selected interatomic distances and bond angles calculated from the parameters, are given in Tables 1 and 2.

In the course of the refinement study, several models for possible nonstoichiometry were tested, including partial substitution for the carbon by the iron, and carbon deficiency. No nonstoichiometry was detected, and the composition of the iron oxycarbonate is therefore stoichiometric $Sr_4Fe_2O_6CO_3$ in agreement with the nominal concentration. The TGA data (Fig. 4) confirm this composition. The TGA data show a weight loss corresponding to a thermal decomposition of 0.970 mole of carbon dioxide per formula unit from the oxycarbonate. The quantity of carbon in the compound found by the thermal analysis is therefore consistent with the formula derived from the ND data analysis.

Each iron ion is coordinated by four in-plane oxygens at 1.976 Å (295 K), and one apical oxygen at 1.904 Å. Two oxygens near the carbon at either 2.61 (to O(C2′)) or 2.95 Å
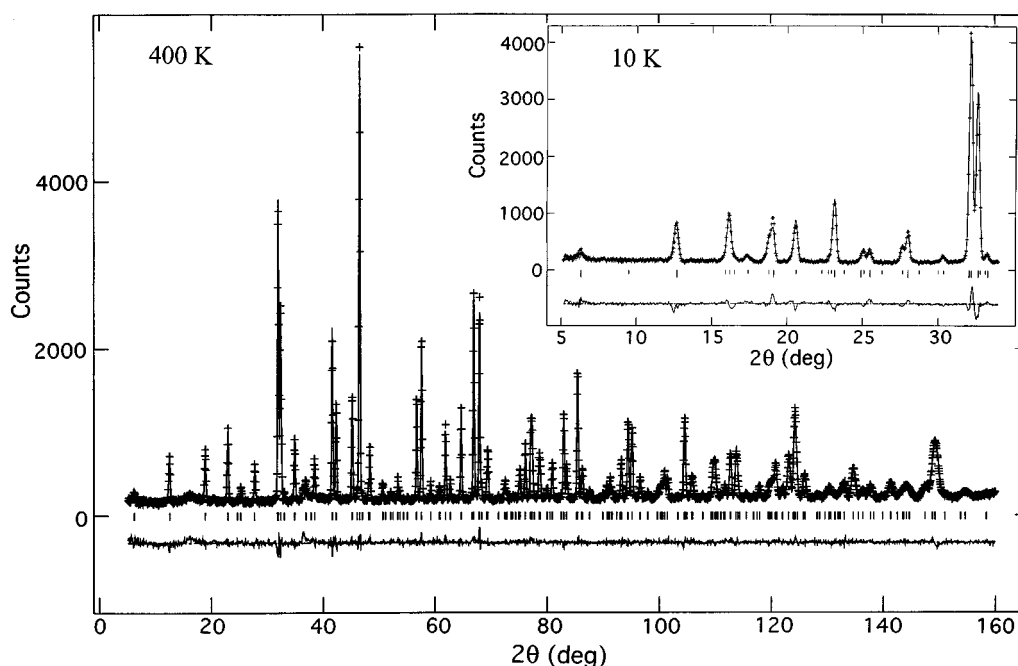

FIG. 2. Plot of the observed (crosses) and calculated (solid curve) powder neutron diffraction profiles at 400 K. The vertical bars indicate the calculated positions for the nuclear Bragg reflections. The lower part of the figure shows the difference between the profiles. The inset shows the low-angle portion of the pattern at 10 K. The positions of the magnetic peaks are indicated by the shorter vertical bars.
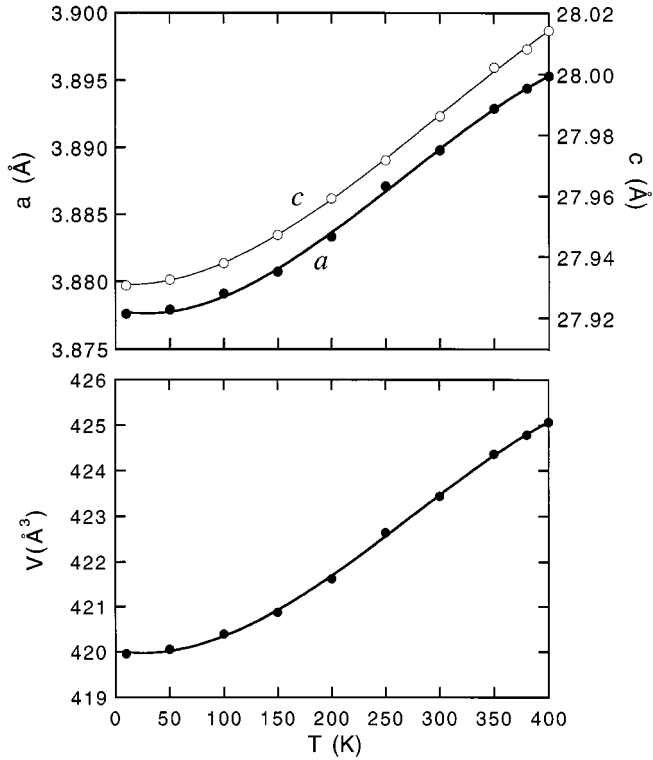
FIG. 3. Plots of lattice parameters and unit cell volume of Sr$_4$Fe$_2$O$_6$CO$_3$ (*I4/mmm*) as function of temperature.

(to O(C2)) are too distant to be considered bonded. The FeO$_2$ layer is not flat. The O(Fe)–Fe–O(Fe) angle is 160 degrees, far from the ideal 180 degrees. Figure 5a shows the locations of the oxygen ions around the carbon, which is a result of eight kinds of orientation of the CO$_3$ triangle (Fig. 5b). Due to constraints on oxygen–oxygen distance, some short-range ordered arrangements of the CO$_3$ triangles that result in distances which are too short (as shown in Fig. 5c) are prohibited from occurring. Further investigation, for example by electron diffraction, could determine whether short-range ordered arrangements of CO$_3$ groups are indeed present.

4. MAGNETIC ORDER

The powder ND patterns for Sr$_4$Fe$_2$O$_6$CO$_3$ indicate that the iron magnetic moments are long-range ordered at low temperature. The temperature dependence of the intensity of the main magnetic peak at $d = 5.5$ Å is shown in Fig. 6. The fit to a mean field model results in an estimate of the long-range magnetic ordering temperature, $T_c = 361(1)$ K. The magnetic Bragg peaks in the patterns were indexed on the basis of a commensurate superlattice with $a_M = b_M = \sqrt{2}a$, and $c_M = c$, where a and c are the lattice parameters of

the chemical unit cell. The inset in Fig. 2 shows the low-angle portion of the pattern at 10 K, where the good fit to the magnetic peaks can be seen. The magnetic structure determined in the refinement study is shown in Fig. 7. The magnetic moments order antiferromagnetically within the FeO$_2$/SrO/SrO/FeO$_2$ block, and ferromagnetically between the blocks. The ordered magnetic moment at 10 K is 3.88(3) μ_B, smaller than that expected for high-spin Fe^{3+} ($3d^5$, $t_{2g}^3 e_g^2$, $S = \frac{5}{2}$). The moments are tilted somewhat from the c_M-axis [24(1) degrees, $\mu_x = 3.53(5)$ μ_B and $\mu_z = 1.59(8)$ μ_B].

5. DISCUSSION AND CONCLUSIONS

The distance between the antiferromagnetic blocks is considerably longer than the in-plane iron-to-iron distance,

TABLE 1
Structure Parameters of Sr$_4$Fe$_2$O$_6$CO$_3$ at 295 K (First Line) and 10 K (Second Line)

Atom	Site	x	y	z	$B(\text{Å}^2)$	n
Sr(1)	4e	0	0	0.29924(5)		1
		0	0	0.29946(4)		1
Sr(2)	4e	0	0	0.42761(5)		1
		0	0	0.42782(5)		1
Fe	4e	0	0	0.14344(4)		1
		0	0	0.14344(4)		1
C	2a	0	0	0		1
		0	0	0		1
O(Fe)	8g	0	0.5	0.13091(4)		1
		0	0.5	0.13061(4)		1
O(Sr)	4e	0	0	0.21149(7)		1
		0	0	0.21122(7)		1
O(C1)	8i	0.346(2)	0	0	1.91(8)	0.125
		0.355(2)	0	0	0.81(6)	0.125
O(C2)	16n	0.159(3)	0	0.0387(4)	1.91(8)	0.125
		0.156(3)	0	0.0331(4)	0.81(6)	0.125
O(C1′)	16n	0.275(3)	0	0.0224(4)	1.91(8)	0.125
		0.273(3)	0	0.0216(4)	0.81(8)	0.125
O(C2′)	4e	0	0	0.0481(2)	1.91(8)	0.25
		0	0	0.0494(2)	0.81(8)	0.25

	B_{11}	B_{22}	B_{33}		B_{11}	B_{22}	B_{33}
Sr(1)	0.79(4)	$(=B_{11})$	0.89(7)	C	1.05(6)	$(=B_{11})$	1.51(9)
	0.10(4)	$(=B_{11})$	0.50(6)		1.17(6)	$(=B_{11})$	1.21(9)
Sr(2)	0.74(4)	$(=B_{11})$	0.96(6)	O(Fe)	0.64(4)	0.49(5)	1.23(6)
	0.56(4)	$(=B_{11})$	0.48(6)		0.60(5)	0.21(5)	0.86(6)
Fe	0.38(3)	$(=B_{11})$	0.65(4)	O(Sr)	1.28(4)	$(=B_{11})$	0.48(6)
	0.36(3)	$(=B_{11})$	0.18(4)		0.64(5)	$(=B_{11})$	0.52(6)

$R_p =$	4.18%		$R_{wp} =$	5.07%	$\chi^2 =$	1.702	
	5.11%			6.26%		2.368	

Note. Space group, *I4/mmm* (No. 139), $z = 2$. The lattice parameters are $a = 3.88907(4)$ Å, $c = 27.9818(4)$ Å at 295 K, and $a = 3.87760(4)$ Å, $c = 27.9309(4)$ Å at 10 K. The temperature factors for the oxygen atoms around the carbon are constrained to be equal.
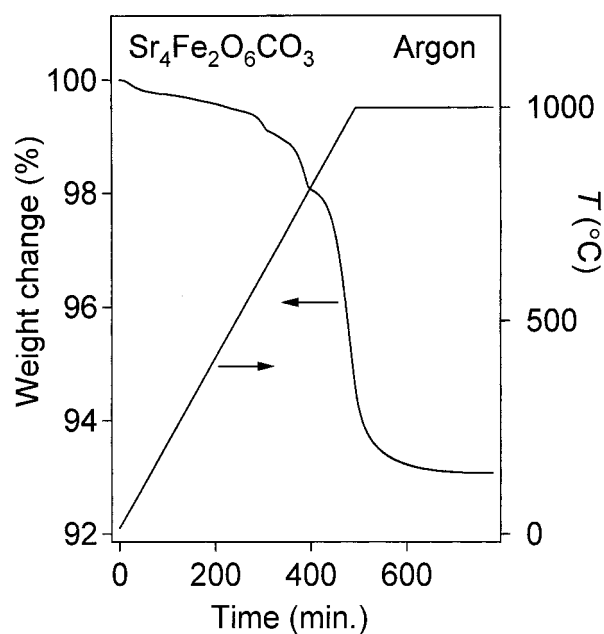
FIG. 4. Thermogravimetric analysis data for a powder sample of $Sr_4Fe_2O_6CO_3$. The weight loss is 6.92%, indicating a quantity of carbon (0.970 mol) per formula unit.

TABLE 2
Selected Interatomic Distances (Angstroms) and Angles (Degrees) for $Sr_4Fe_2O_6CO_3$

Atoms		295 K	10 K
Sr(1)–O(Fe)	×4	2.757(1)	2.752(2)
Sr(1)–O(Sr)	×1	2.455(2)	2.469(2)
Sr(1)–O(Sr)	×4	2.7663(2)	2.7581(2)
Sr(2)–O(Fe)	×4	2.542(1)	2.534(1)
Sr(2)–O(C1)	×1	2.871(2)	2.853(2)
Sr(2)–O(C2)	×1	2.536(7)	2.594(7)
Sr(2)–O(C1′)	×1	2.551(8)	2.555(8)
Sr(2)–O(C2′)	×1	2.833(2)	2.815(1)
Fe–O(Fe)	×4	1.9759(3)	1.9716(3)
Fe–O(Sr)	×1	1.904(2)	1.893(2)
Fe–O(C2)	×0.5	2.946(8)	3.14(1)
Fe–O(C2′)	×0.25	2.609(9)	2.626(1)
C–O(C1)	×0.5	1.344(8)	1.376(8)
C–O(C2)	×1	1.25(1)	1.11(1)
C–O(C1′)	×1	1.24(1)	1.22(1)
C–O(C2′)	×0.5	1.346(6)	1.381(5)
O(Fe)–Fe–O(Fe)		159.57(9)	159.06(9)
O(Fe)–Fe–O(Fe)		88.20(2)	88.11(2)
O(Fe)–Fe–O(Sr)		100.22(5)	100.47(5)
O(C1)–C–O(C2)		119.6(5)	123.3(6)
O(C2)–C–O(C2)		120.7(9)	114.4(12)
O(C1′)–C–O(C2′)		120.3(5)	119.6(5)
O(C1′)–C–O(C1′)		119.3(11)	120.8(11)

and therefore two-dimensional magnetic anisotropy is expected. The perovskite-type compounds $RFeO_3$ ($R =$ La–Lu) have a three-dimensional network of antiferromagnetic (Fe^{3+})–(O^{2-})–(Fe^{3+}) bonds, where the bond angle is between 158 (La) and 140 (Lu) degrees. The Néel temperatures are high, between 700 (La) and 580 (Lu) K (7). This suggests that two-dimensional antiferromagnetic ordering in the FeO_2 layers in $Sr_4Fe_2O_6CO_3$ may exist above the
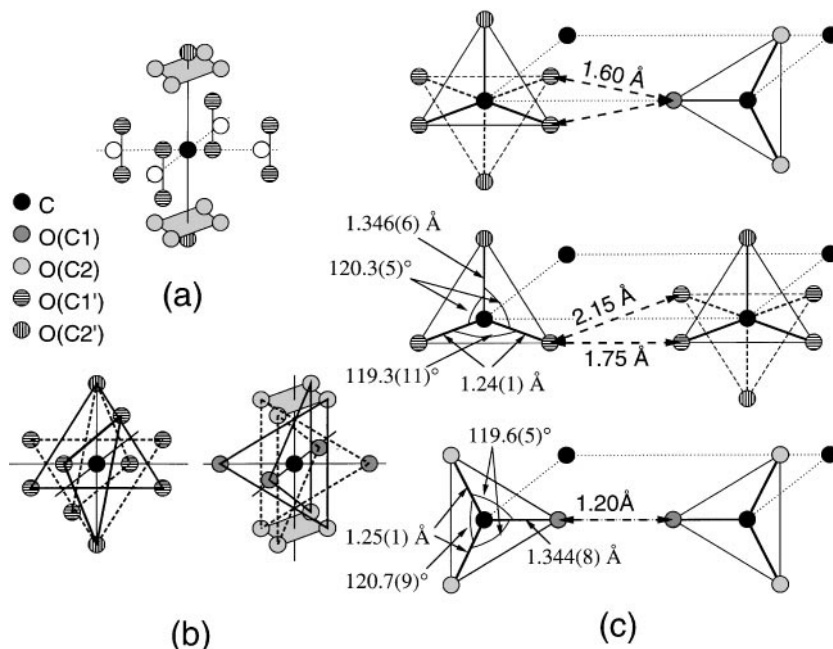

FIG. 5. (a) Positions for the oxygen atoms around the carbon. (b) Possible orientations of the CO_3 triangular plaques. (c) The CO_3 triangle arrangements that should not occur due to short oxygen-to-oxygen distances.
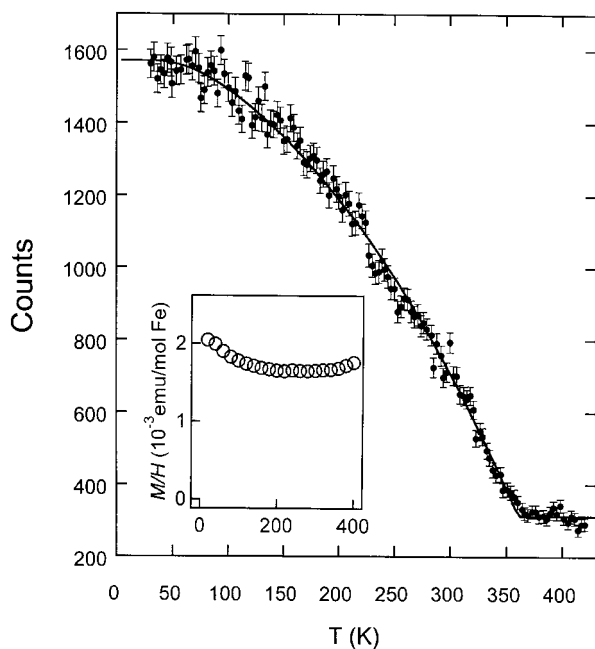
FIG. 6. Peak intensity of the (0.5, 0.5, 0) magnetic reflection (referred to chemical cell) as a function of temperature for $Sr_4Fe_2O_6CO_3$, indicating a T_c of 361(1) K. The solid curve is a mean-field fit to the data. The inset is the magnetic susceptibility data for $Sr_4Fe_2O_6CO_3$ measured at 90 kOe.
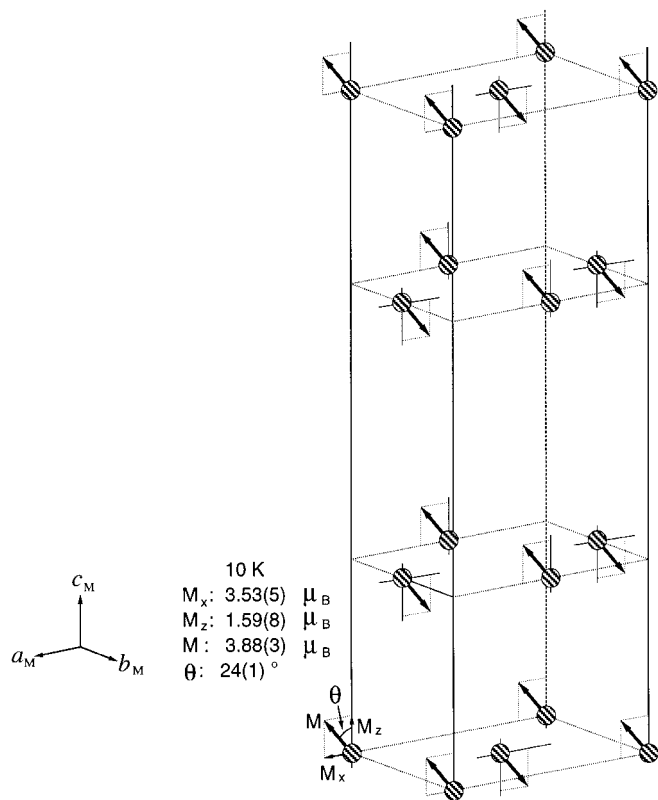
three-dimensional ordering temperature. We found that the development of short-range magnetic fluctuations becomes significant above approximately 250 K, making fits to the magnetic peaks problematical. For example, the tilt angle of the moment seems to increase slightly from 24 degrees with increasing temperature, but it is difficult to follow precisely due to the consequent broadening of the peaks and inclusion of inelastic magnetic scattering. The anisotropy in the magnitude of the magnetic correlation, relatively weaker along the c-axis than in the FeO_2 layer, may be the origin of the unusual magnetic susceptibility data (inset in Fig. 6).

FIG. 7. Magnetic structure at 10 K for $Sr_4Fe_2O_6CO_3$, where $a_M = b_M = \sqrt{2}a$, and $c_M = c$ (a and c are the lattice parameters of the tetragonal crystal structure).
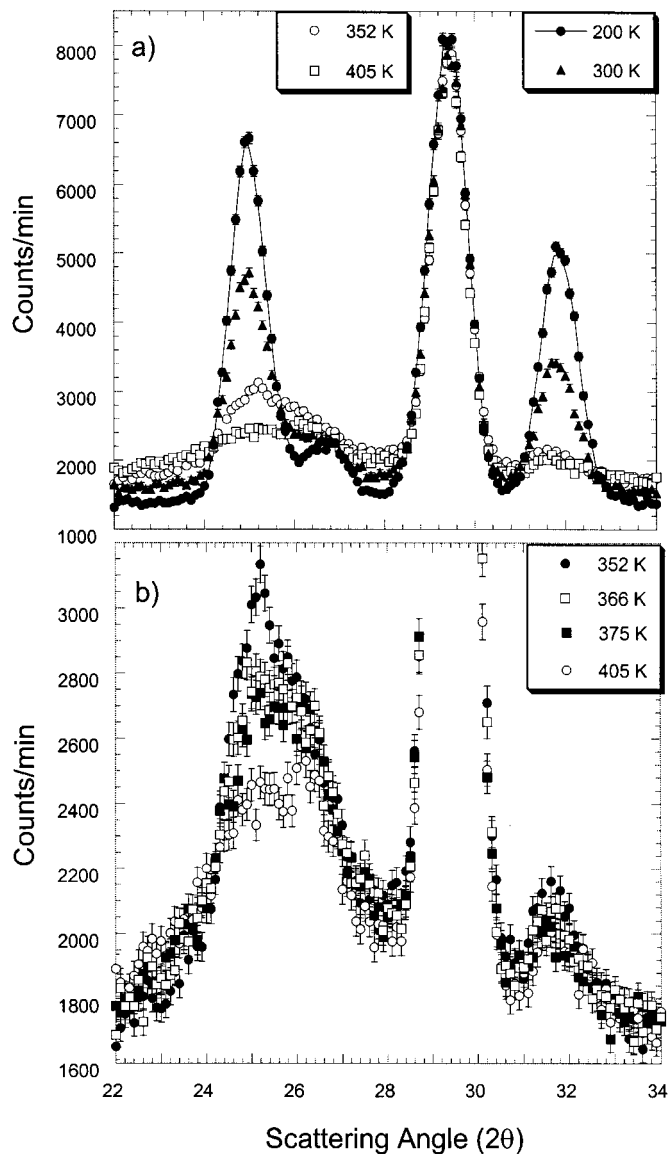

FIG. 8. (a) Evolution of the magnetic scattering with temperature increasing through the T_c of 361 K. At 200 K the peaks are sharp, while at 300 K and higher there is substantial inelastic scattering, broadening the magnetic peaks and skewing the distribution. (b) Vertical scale expansion with additional data at slightly above T_c (366 and 375 K).

The evolution of the magnetic scattering was studied (Figs. 8a and 8b) as a function of temperature in the higher temperature regime. The data were taken between 22 and 34 degrees in scattering angle. The peaks at the left and right of the peak at 29.5 degrees are of magnetic origin. At 300 K substantial inelastic scattering is apparent. Figure 8b clearly shows the evolution near T_c; the peaks broaden and the scattering becomes skewed to higher angles, as expected for a low-dimensional system (8). A careful inspection of the powder ND pattern at 400 K (Fig. 2) also reveals that substantial magnetic correlations persist, although the pattern was taken above the three-dimensional ordering temperature. The sharp sawtooth profile of scattering expected from an ideal two-dimensional magnet was not observed clearly (8). Further study of the magnetic susceptibility and neutron scattering on single crystals of $Sr_4Fe_2O_6CO_3$ would be of interest to clarify the magnetic properties of this phase.

REFERENCES

1. M. Imada, A. Fujimori, and Y. Tokura, *Rev. Mod. Phys.* **70,** 1039 (1998).
2. C. Brisi and P. Rolando, *Ann. Chim.* (*Rome*) **59,** 385 (1969).
3. E. Takayama-Muromahi, *Chem. Mater.* **10,** 2686 (1998).
4. T. Seguelong, P. Maestro, J.-C. Grenier, L. Fournes, and M. Pouchard, *Physica B* **215,** 427 (1995).
5. V. Caignaert, Ph. Daniel, N. Nguyen, A. Ducouret, D. Groult, and B. Raveau, *J. Solid State Chem.* **112,** 126 (1994).
6. A. C. Larson and R. B. Von Dreele, Los Alamos National Laboratory Report No. LAUR086-748, 1990.
7. I. S. Lyubutin, T. V. Dmitrieva, and A. S. Stepin, *Zh. Eksp. Teor. Fiz.* [*Sov. Phys. JETP*] **88,** 590 (1999).
8. J. W. Lynn, *J. Alloys Compds.* **181,** 419 (1992).